



## Research paper

# Design and Fabrication of Hemispherical Shell Resonator by Glass Blowing Method

A. Khooshehmehri\*, A. Eslami Majd, S.A. Hosseini

Faculty of Electrical and Computer, Malek-Ashtar University of Technology, Tehran, Iran.

## Article Info

### Article History:

Received 03 January 2021

Reviewed 20 February 2021

Revised 16 March 2021

Accepted 24 April 2021

### Keywords:

Hemispherical resonator gyroscope

Hemispherical shell resonator

Glass blowing method

MEMS technology

Crystallization

\*Corresponding Author's Email Address:

[khooshehmehri@mut.ac.ir](mailto:khooshehmehri@mut.ac.ir)

## Abstract

**Background and Objectives:** The Hemispherical Resonator Gyroscope (HRG) has been a valuable choice for the aerospace industry due to its low noise, good performance, and long lifetime. Its main part consists of a hemispherical shell resonator (HSR). Recently, with the idea of using MEMS technology and using materials such as Pyrex in the construction of HSR, a significant reduction in the size, weight, and power consumption of this gyroscope along with the special gyroscopic characteristics of HRG, Today, and the Micro-HRG has been introduced as a sensor in the strategic class.

**Methods:** Micro-HSR can be implemented in three ways: micromachining, blowtorching, and glass blowing. In this paper, after a brief introduction and comparison of possible approaches to make an HSR, the glass blowing method is selected and the sub-processes of this method are introduced and the results of its implementation are presented.

**Results:** The proposed sensor is made by performing the glass blowing method, with a radius of 1.536 mm, a middle base radius of 252  $\mu\text{m}$ , and a shell height of 355  $\mu\text{m}$ . Also, the most important fabrication parameters for achieving the desired geometrical shell were as follows: The appropriate initial thickness of Pyrex is 200  $\mu\text{m}$  and the depth of the cavity under the silicon layer is 532  $\mu\text{m}$ . The bonding process to create a stable connection between Si and Pyrex must be performed at a voltage of 800 V and at a temperature of 550  $^{\circ}\text{C}$  for 30s. In addition, the blowing process with a heating rate of 4  $^{\circ}\text{C}/\text{s}$  and a cooling rate of 9.5  $^{\circ}\text{C}/\text{s}$  has been evaluated as a suitable thermal profile. By optimally controlling the temperature process in the blowing sub-process, the crystallization phenomenon is prevented, which will lead to the improvement of the HSR quality factor.

**Conclusion:** Achieving the technology of making this hemispherical glass shell in sub-millimeter dimensions, which plays the role of the resonator in an HRG, due to the superior features of this gyroscope such as low noise, good performance, and long lifetime and its application in strategic industries, like navigation and smart weapons, it is of particular importance.

©2022 JECEI. All rights reserved.

## Introduction

Resonator gyroscopes operate on the basis of the law of conservation of momentum. The resonator gyroscope consists of three main parts: resonator shell, interface electrodes, and control circuits, and based on the

structure of the resonator shell, they are classified into different types such as fork, cylindrical, annular, planar, and hemispherical resonator gyroscopes [1].

The function of a hemispherical resonator gyroscope is such that by exciting the resonator shell, a standing

wave vibrates on it, and in proportion to the resonance mode of this wave, a number of nodes and antinode are created on the shell. Applying input to the gyroscope and rotating the shell around its axis causes the Coriolis force to be applied to the standing wave [2]. By applying Coriolis force and standing wave displacement, the position of the nodes and antinodes changes and creates a quadrature wave. The result of the main wave and the quadrature wave creates a new wave. The amount of angular displacement of this new wave relative to the initial standing wave at any given moment is proportional to the amount of input rotation angle of the shell. The amount of standing wave movement is transmitted through the interface electrodes to the control circuits and the control circuits calculate the input rotation angle [3]-[5].

A resonator gyroscope in which a hemispherical resonator shell is a bed of standing waves is called an HRG. HRG is the only type of resonator gyroscope in the navigation class [3] and is known as one of the most accurate gyroscopes in inertial navigation [6]. This is due to the spatial symmetry of HSR and the significant reduction of energy losses in this structure, which improves the gyroscopic characteristics such as precision, sensitivity, performance accuracy, and error in measuring the angle. Among millimeter-dimension gyroscopes, HRG has the best angle random walk value and bias stability [4]. Another important advantage of this gyroscope is its resistance to external vibrations due to the integrity of its sensor structure. In other words, the lack of a moving part in the sensor structure of this gyroscope makes it resistant to many influential environmental variables and has the ability to operate for a long time without the need for maintenance [7]. Due to the superior features of HRG, its application in guidance and navigation sensor systems is increasing [8], [9].

The idea for this type of gyroscope, based on the displacement of a standing wave in proportion to the resonator input rotation, was proposed by Bryan in 1982 and published in the Journal of the University of Cambridge [10]. After implementing the idea of an HRG, this gyroscope has been used in a variety of space missions since 1996. The use of this type of gyroscope by NASA and the European Space Agency in the Cassini spacecraft (1997-2017) is considered one of the most important missions of the HRG. The HRG gyroscope was also used in the Messenger spacecraft (2004-2015). The spacecraft was built by NASA to orbit Mercury, and its mission was to identify the chemical materials, climate, and magnetic field on Mercury [4]. This type of gyroscope has also been used in cases such as stability and guidance of missiles and smart ammunition in the military industry [7]. Due to the successful results of HRG

in various missions, the function of this gyroscope has been proven as a reliable technology for use in air, space, and military applications [11].

As the types of flying and moving objects get smaller and lighter, one of the most important characteristics of choosing a sensor system is its size, weight, and power consumption. HRG, despite the very desirable gyroscopic characteristics in the navigation class, due to the large size and material of the resonator shell and consequently the size of the electrodes and interface circuits, in some applications was gradually replaced by various optical gyroscopes. Gyroscopes that although did not have the accuracy, longevity, and stability of HRG, were more appropriate in terms of weight and size. With the growth of MEMS technology and the idea of using this technology in the construction of HRG, the effort to take advantage of high accuracy, reliable performance, and low error of these gyroscopes in various flying and moving objects in the field of air, space and earth began. Initially, HRG micro-scale specimens were not popular due to their three-dimensional lithography stage in the micromachining HSR fabrication process and the need for a complex circuit to amplify the signal. These limitations have been overcome in recent years with innovations in manufacturing processes and equipment, and the HRG micro-scale specimen has been introduced as an angular rate integration gyroscope [12], [13]. Some of the important advantages of these gyroscopes, which have attracted researchers in the field of rockets and aerospace: [2]

1. Have a short start time.
2. Due to the lack of rotor shaft, they do not need bearings.
3. No engine required.
4. Their lifespan is very long and does not need maintenance.
5. They are much smaller and lighter than traditional gyroscopes
6. It is relatively easier to build.
7. Very low energy consumption.

Micron-sized HSR is made using MEMS technology and in three ways: glass blowing, blow torching, or micromachining. Recently, research on the construction of this type of gyroscope in micron dimensions and increasing its quality characteristics along with reducing weight and size and power consumption has been expanded [4]. In 2007, Andrei Shkel et al. reported for the first time the construction of several HSRs simultaneously in a way other than the conventional micromachining method [14]. In the last decade, a 2014 report published by the Department of Defense Research Institute identifies micro-scale shells made by Professor Khalil Najafi of the University of Michigan and Professor Andrew Shall at the University of California

[15]. In 2017, Asadian presented a report on the construction of a hemispherical shell by blowing glass, which was supported by the US Department of Defense Research Institute [16]. In 2020, Yoong Cho et al. reported HSR construction with an improvement in the quality factor of about 5.2 million and an ARW parameter of 0.00016 deg / (vh) [17]. In this paper, the construction of an HSR in micron dimensions is reported. For this purpose, the existing implementation techniques were reviewed and the glass blowing technique was selected. After selecting the appropriate method, for each of the sub-processes of this technique, the fabrication parameters of each sub-process are designed and implemented.

These sub-processes include the etching of cavities, the Pyrex bond to the substrate, and the blowing process. Among the most important fabrication parameters that are studied in this research and its values are stated in the article include Pyrex thickness, Depth of cavity, temperature, and voltage of the bonding stage to achieve a suitable and strong connection and temperature profile in the blowing stage.

The heating and cooling rate of the sample is very important in the correct formation. Also, the crystallization of the resonator shell is prevented by optimal control of the temperature process in the cooling stage. In this paper, after introducing the conventional methods for making a micro-scale HSR, focusing on the glass blowing method, its parameters and sub-processes are described according to the desired design. In the end, samples are made and the results are presented.

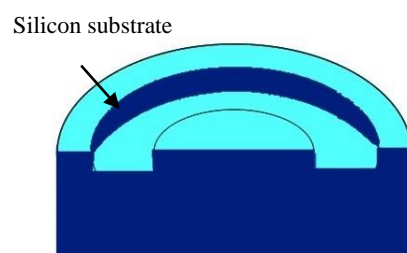
### HSR Fabrication Methods

Glass blowing, blow torching, or micromachining methods can be used to make the resonator shell of the HRG gyroscope in micro dimensions. In the glass blowing method, after selecting the appropriate substrate, a hole is created on the substrate using etching processes. The substrate and the glass layer are then bonded together and the air is trapped inside the cavity. Then, using a suitable heating process, the blowing process takes place by expanding the gas inside the cavity at the same time as the glass reaches the softening temperature. At this stage, a hemispherical structure is obtained by forming the glass layer [5]. The surface tensile force in this process creates high symmetry and minimal surface roughness [18], [19]. In the blow torching method, a layer of glass is placed between two prefabricated graphite molds. By applying point temperature from above and pressure difference from below the molds, the glass layer is deformed and pulled into the cavity.

This process is performed in a short time using a centralized burner with a temperature of about 2500 ° C, which is higher than the melting point of used glass such

as fused silica [20]–[22]. In the micromachining method, the desired shell is made by performing several sub-processes, which include several stages of lithography and very precise and complex etching [23]. Therefore, the construction of HSR with proper symmetry and roughness by the micromachining method requires very precise and special construction facilities and equipment. A comparison of HSR implementation methods is given in Table 1. The glass blowing method and the blow torching method are both based on surface tension, so the shell has fewer structural defects than the micromachining method [24]. Making shells in these two methods is simpler than the micromachining method and has fewer sub-processes [25]–[28] and very important advantage in these two methods is the possibility of making shells in a common process and simultaneously. Which provides access to resonators with very similar characteristics [25]–[29]. Although the blow torching method makes it possible to achieve larger dimensions, for reasons such as limitations in the design of the resonator stem, the need for high accuracy in aligning the center of the burner with the center of the mold [25] and the need to apply concentrated heat in proportion to the melting point temperature of the material faces limitations in design and implementation [25]. As mentioned, the maximum heat required to perform the temperature process in the glass blowing method determines the softening point temperature of the glass layer [29]. While the maximum temperature of the temperature process in the blow torching method is determined by the temperature of the melting point of the material [26]. One of the most important features of the glass blowing method, in addition to lower manufacturing costs [30], is the symmetry and roughness of the resulting shell surface.

The reason for this is the formation of the shell during a natural process without the involvement of tools or molds in the formation of the final structure of the shell. Thus, according to the comparison between the existing methods, the glass blowing method was selected to make the shell in this article. This method consists of three main stages, which include the cavity formation stage, the bonding stage, and the blowing stage. Fig. 1 shows the main steps of the glass blowing process.



(a)

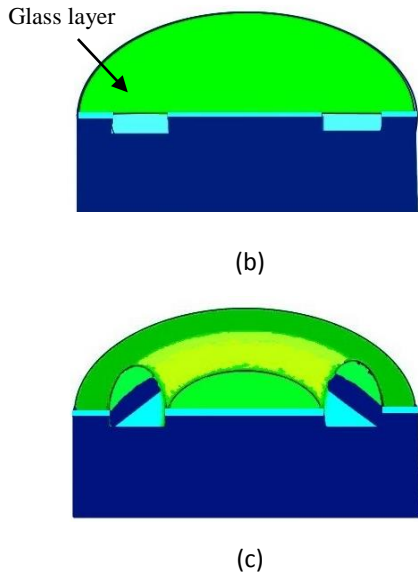


Fig. 1: Steps of glass blowing process. (a) Creating a hole in the silicon substrate, (b) bonding the glass layer with a silicon substrate, (c) blowing the glass layer.

**A. The Stage of Creating a Cavity**

The purpose of this step is to create a cavity in the substrate. A cylindrical cavity in which the smoothness and uniformity of the edges and the symmetry of the opening are important.

**B. The Bonding Stage**

In the bonding stage, a layer of glass is attached to the substrate so that the air inside the cavity is trapped. The integrity and strength of the two-layer bond at the junction are of great importance.

**C. The Blowing Stage**

During the blowing process, the substrate and the bonded layer are subjected to a heat process up to the softening temperature of the glass. In this process, the surface tension of the glass on the one hand and the expansion of the air inside the cavity on the other hand cause the deformation of the glass layer. This blowing process continues until the pressure inside the shell equals the external pressure of the environment. During this stage, the tensile force at the atomic scale at the surface of the shell structure minimizes surface roughness and structural defects.

Table 1: Comparison of HSR implementation methods

Fabrication method	Surface tension		Micromachining
	Glass blowing	Blow torching	
<b>Advantages</b>	1) Simplicity of implementation of the manufacturing sub-processes 2) Low construction cost 3) Less structural defects 4) Better symmetry and smoothness of the shell surface 5) Possibility of making HSR with Pyrex, borosilicate glass, titanium silicate glass and quartz 6) Ability to build multiple rows of vibrating shells simultaneously	1) Possibility of shell formation in a short time (about five to twenty seconds) 2) Ability to adjust the height of the shell with designing the mold 3) Possibility of using fused silica in making HSR 4) Flexibility in design 5) Low construction cost 6) The temperature in this process rises to 2500 degrees, which is higher than the melting point of many high quality materials.	1) Ability to fine-tune the dimensions of the shell 2) It is possible to make a shell with materials such as diamond, which due to its high strength and low thermal expansion coefficient, provides HSR with a better quality coefficient. 3) Ability to make shells with less thickness
<b>Limitations</b>	1) It is difficult to make a shell with this method, with large dimensions. 2) The geometry of the crust is affected by the photolithographic pattern and the dimensions of the cavity. 3) It is difficult to use fused silica with a softening temperature of about 1585 degrees.	1) In this method, the structure with hollow stem can be obtained, but the structure with solid stem cannot be created. 2) In this method, the burner and the mold must be exactly aligned to prevent unevenness and imbalance in the temperature distribution, which aligns the center of the burner with the center of the mold requires very high accuracy. 3) The height of the shell cannot be changed without changing the shape of the mold. 4) High sensitivity to rate of shell height changes over time.	1) Impossibility to adjust the height of the shell 2) The length of the stem is smaller than the height of the shell 3) Dangerous and scarce materials used in the manufacturing process 4) Costly and time consuming laboratory process
<b>References</b>	[14], [29], [31]–[35]	[20], [25], [32], [36]–[39]	[39]–[43]

HSR fabrication design section explains the relationship between geometric parameters and fabrication parameters in the glass blowing process. In the Glassblowing technique Implementation section, the implementation of its sub-processes is detailed. One of the most important points to be considered in the glass blowing method is the dependence of the geometry of the shell on the dimensions of the cavity [29] and also the design of an appropriate temperature process to prevent the crystallization of the shell [26].

**HSR Fabrication Parameters**

The HSR in the HRG gyroscope is the base for standing wave formation and so far it has been designed and implemented with various structures. These structures are divided into three general categories based on the geometry of the shell and its anchor: wineglass gyro, mushroom gyro, and quasi-spherical gyro. In the quasi-spherical structure, the hemisphere opening is downward and has a circumferential anchor. In this structure, the edge of the hemispherical shell acts as an anchor. In the other two structures, the anchor is axial, as the hemispherical shell is on the middle stem, which acts as the anchor of the shell. The difference between the wineglass and mushroom structures is in the direction of the hemispherical shell. In the wineglass structure, the hemispherical shell opening is upward and in the mushroom structure, the hemispherical shell opening is downward. Fig. 2 shows a schematic of the various shell structures.

The wineglass structure is seen in Fig. 2 (a) is the first structure considered in the design of HRG. The wineglass structure is less resistant to sudden shocks than other structures. This structure is usually made by the micromachining method. The wineglass structure can also be made by blowing glass or blow torching, in which case it is necessary to set the hemispherical shell with very high precision on a prefabricated stem.

Another structure that can be seen in Fig. 2 (b) is the quasi-spherical structure. This structure has a very high strength for shocks and sudden shocks due to its environmental anchor. Due to the adhesion of the hemisphere edge, this structure is not very sensitive. The quasi-spherical shell is usually implemented by the glass blowing method, and the electrode process for this structure is usually performed during the glass blowing process. One of the challenges of making a quasi-spherical shell is the need to achieve a structure with a height to radius ratio greater than 1. Fig. 2 (c) shows a schematic of the mushroom shell structure. The mushroom shell, on the one hand, has good resistance to unwanted environmental shocks and vibrations, and on the other hand, provides the necessary sensitivity for the sensing mission. The mushroom structure can be

implemented by glass blowing and micromachining methods.

By examining the structures and comparing the features and considering the quality factor and sensitivity and fabrication challenges, the mushroom structure was selected for implementation. After selecting the appropriate structure, the shell fabrication process is designed by examining the relationships between the fabrication parameters and the geometric characteristics of the mushroom shell. The geometric parameters of the mushroom shell are shown in Fig. 3.

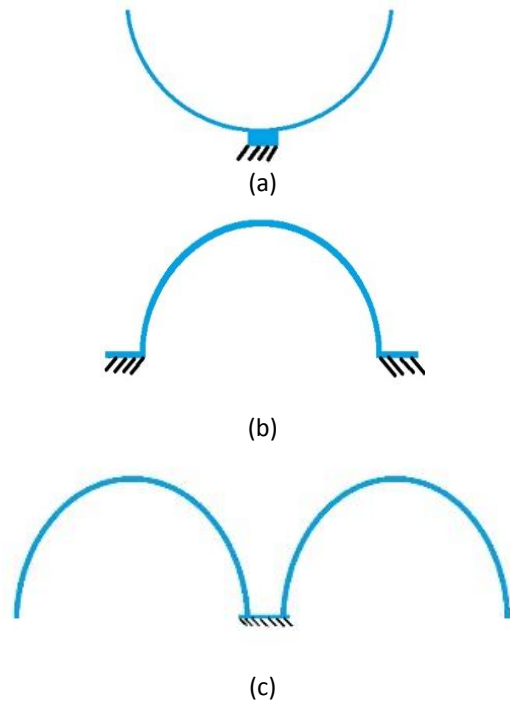


Fig. 2: Schematics of the various shell structures. (a) The wineglass structure, (b) the quasi-spherical structure, (c) the mushroom shell structure.

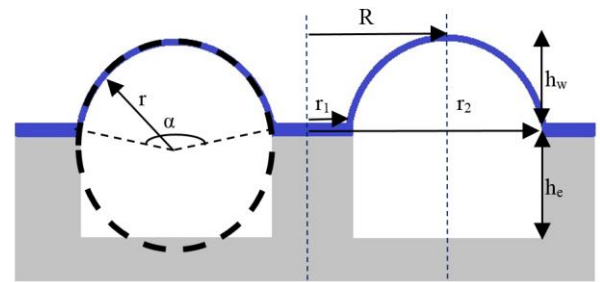


Fig. 3: Scheme of the shell with mushroom structure and geometric parameters of the shell.

As shown in Fig. 3, the smaller radius  $r$ , the larger radius  $R$ , the inner circumference radius  $r_1$ , the outer circumference radius  $r_2$ , the etching depth  $h_e$ , and the hemispherical height  $h_w$  are given. First, according to Fig. 3, the volume of the etching hole is calculated using (1):

$$V_{cavity} = \pi \cdot (r_2^2 - r_1^2) h_e \tag{1}$$

In (1),  $r_2$  is the outer radius of the cavity,  $r_1$  is the inner radius of the cavity and  $h_e$  is the depth of the cavity. After heating, the air inside the cavity expands to form the desired mushroom shell. The resulting shell volume can be calculated using the ideal gas law from (2):

$$V_{shell} = \left(\frac{T_f}{T_i} - 1\right) \cdot V_{cavity} \tag{2}$$

In (2), the temperatures  $T_i$  and  $T_f$  are expressed in Kelvin. These temperature characteristics correspond to the temperature at the beginning and end of the glass blowing process, respectively. Also, the air pressure inside the cavity and the air pressure inside the furnace chamber is assumed to be equal to the atmospheric pressure [35]. Using geometric parameters, the shell volume can be obtained from (3):

$$V_{shell} = \pi \cdot R \cdot r^2 \cdot (\alpha - \sin \alpha) \tag{3}$$

In (3),  $\alpha$  is the central angle of the arc formed by the partial radius. Small and large radii can be obtained using (4) and (5):

$$r = \frac{r_2 - r_1}{2 \cdot \sin\left(\frac{\alpha}{2}\right)} \tag{4}$$

$$R = \frac{r_2 + r_1}{2} \tag{5}$$

Also, the height of the shell ( $h_w$ ) can be calculated based on the smaller radius ( $r$ ) and the angle arc parameter ( $\alpha$ ) from (6):

$$h_w = r \cdot \left(1 - \cos\left(\frac{\alpha}{2}\right)\right) \tag{6}$$

These Equations are based on the glass blowing process and the geometry of the mushroom shell in micro-scale dimensions.

### Glassblowing Technique Implementation

After selecting the glass blowing method in order to make an HSR with mushroom structure, fabrication parameters and necessary sub-processes were designed and implemented. In this article, how to implement the steps of making the shell by glass blowing is as follows.

#### A. The Stage of Creating a Cavity

A P-type silicon wafer with a thickness of 700  $\mu\text{m}$  has been selected as the substrate. In the first stage, using the CNC process, a hole was created on the silicon substrate with an outer radius of 1536  $\mu\text{m}$  and a depth of 532  $\mu\text{m}$ . The roughness of the cavity opening was then reduced to less than 5  $\mu\text{m}$  during the RIE process.

#### B. The Bonding Stage

At this stage, the connection of the Pyrex 7740 layer with a thickness of 200  $\mu\text{m}$  on the silicon substrate has

been done by an anodic bonding method. The Pyrex and silicon layers are adjusted to each other in a proper position after the RCA cleaning step and are bonded together during the end bonding process: at a voltage of 800 V at a temperature of 550  $^{\circ}\text{C}$  for 30 seconds.

#### C. The Blowing Stage

In order to perform the blowing stage and the formation of the shell in this stage, the connected sample of silicon and Pyrex is subjected to a special heat process inside the furnace. The temperature of the furnace in the glass blowing process is determined according to the softening point of Pyrex. At this stage, the furnace is set at a temperature of 880 $^{\circ}\text{C}$ . During the blowing process, the instantaneous temperature of the process is very influential in how the shell is formed, the resulting dimensions, the geometric symmetry of the shell, and the non-crystallization of the Pyrex layer. According to the studies, the temperature process in this stage has been done according to the diagram of Fig. 4.

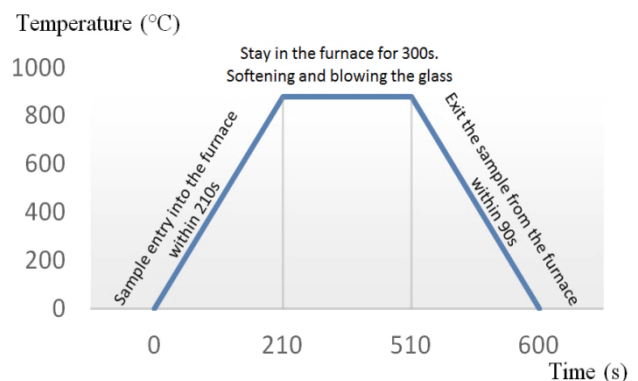


Fig. 4: Temperature profile diagram of blowing process.

Table 2: Implementation parameters of the HSR fabrication process with glass blowing method

The roughness of the cavity opening ( $\mu\text{m}$ )	The cavity depth ( $\mu\text{m}$ )	The outer radius of the cavity ( $\mu\text{m}$ )	The inner radius of the cavity ( $\mu\text{m}$ )	Thickness of silicon ( $\mu\text{m}$ )	The cavity etching stage
5	532	1536	252	704	
Duration time	Voltage	Temperature			The bonding stage
30s	800V	550 $^{\circ}\text{C}$			
Sample Exit time	Sample remain time	Sample entry time			The blowing stage
90s	300s	210s			

In the steps mentioned in the implementation of the glass blowing method, key parameters such as cavity volume, uniformity of cavity edges, bonding voltage and

temperature, maximum furnace temperature and entry and exit speed and stopping time of the sample in the furnace are determined and adjusted in the appropriate range and a hemispherical shell with a mushroom structure was made. Finally, after the steps of making the shell with the specifications given in Table 2, the HSR with mushroom structure was made.

## Results and Discussion

Mushroom shell made of Pyrex 7740 on a silicon substrate. The evaluation of the shell characteristics is done with intermediate tests during the manufacturing process and after the complete execution of the manufacturing steps. Intermediate assessments include measuring the cavity volume and the uniformity of the cavity opening, which determines the final shell volume and the roughness of the final shell surface. After the bonding stage, the accuracy and the uniformity of the bond are evaluated by examining the Newtonian rings with an optical microscope. Also at this stage, another sample that is made at the same time as the original sample (control sample) is subjected to destructive testing to evaluate the strength of bonding quality. After blowing the sub-process, the final shell characteristics such as geometric dimensions, symmetry, and roughness of the shell surface are examined using an optical microscope and SEM test. Fig. 5 shows an SEM image of an HSR sample made with a mushroom structure consisting of a glass shell with a middle stem on a silicon substrate.

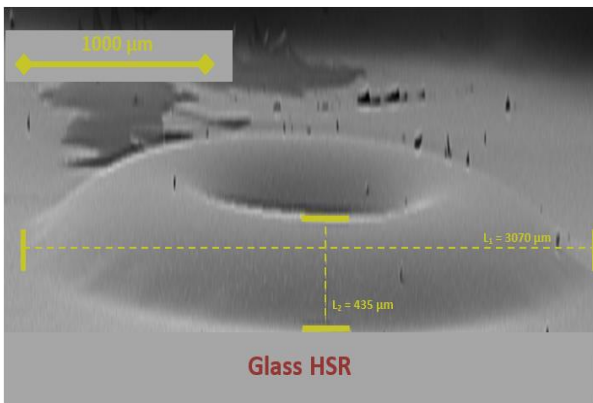


Fig. 5: SEM image from an unequal angle of a mushroom structure HSR on a silicon substrate by the glass blowing method. This image displays the 3D shape of the shell.  $L_1$  is twice the outer radius and  $L_2$  is the width of the shell from an unequal angle.

This hemispherical shell image shows that the shell does not crystallize and also shows the correctness of the glass blowing sub-processes and the overall geometry of the shell. The SEM image of the side view of the sample is shown in Fig. 6.

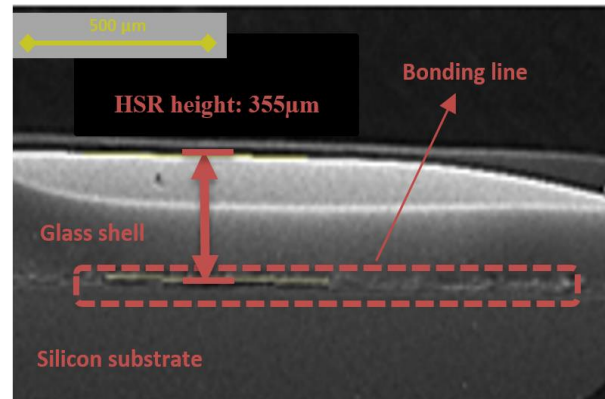


Fig. 6: SEM image from the side of the HSR with a mushroom structure with a height of 355  $\mu\text{m}$  on a silicon substrate made by blowing glass.

The side view image is examined to check the height of the shell. As can be seen in the SEM image from the side in Fig. 6, the glass shell increased uniformly during the blowing stage and grew to a height of 355  $\mu\text{m}$ . In the image from the side of the sample, in addition to measuring the height of the shell, the accuracy of the anodic bonding process is also confirmed by showing the boundary of the silicon and Pyrex area. Fig. 7 shows the SEM image from the top of the constructed sample. The SEM image from above shows the symmetry of the shell.

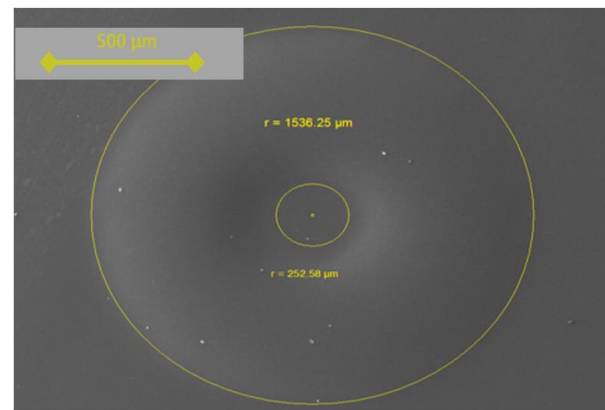


Fig. 7: SEM image from the top of the HSR with a mushroom structure. The outer radius of the shell is 1536.25  $\mu\text{m}$  and the inner radius is 252.58  $\mu\text{m}$ .

Also, using this image, the HSR created radius and the middle stem radius can be measured. Another important feature of the shell that can be seen in the image from above is the symmetry of the glass shell. The symmetry of the glass shell depends on the quality of the manufacturing process. In the silicon cavity formation stage, symmetry in the circular shape of the cavity opening and smoothness of the cavity edge is very important.

Also, the uniformity and strength of the bonding at the edge of the cavity on the one hand and the uniform conditions of the furnace for all sample points in the blowing stage on the other hand are effective factors in creating a symmetrical shell. If any of these steps are not performed correctly, an asymmetric increase in volume will be detected in the image from above. In the measurements obtained from the SEM image from above, the outer radius of the HSR was 1536  $\mu\text{m}$  and the inner radius of the HSR was 252  $\mu\text{m}$ . The results of sample measurements are shown in Table 3.

Table 3: Measurement results of the fabricated HSR sample

Final HSR characteristics				Bonding quality		Cavity parameter
Radial symmetry	Inner radius of the HSR	Outer radius of the HSR	HSR height	destructive test	Newtonian rings	Cavity volume
✓	252 $\mu\text{m}$	1536 $\mu\text{m}$	355 $\mu\text{m}$	✓	✓	2.5mm <sup>3</sup>

## Conclusion

In this paper, a laboratory sample of a glass hemispherical shell with a mushroom structure and glass blowing method is reported.

This method is performed by implementing three main sub-processes, including the creation of a cavity in the silicon substrate, the Pyrex thin-layer bond to the silicon substrate, and finally the blowing in the high-temperature furnace.

By designing the mentioned sub-processes and finding the desired working point, a glass shell with a hemispherical structure with a stem and by controlling the crystallization in its crystal structure was obtained. As mentioned, the desired shell was made by blowing glass, with an outer radius of 1,536 mm, an inner radius of 252  $\mu\text{m}$ , and a shell height of 355  $\mu\text{m}$ . For this purpose, a Pyrex 7740 with an initial thickness of 200  $\mu\text{m}$  was used and the depth of the cavity in the Si layer was considered to be 532 micrometers.

The bonding sub-process was performed at a voltage of 800 V and at 550 ° C for 30 s to create a strong connection between Si and Pyrex that has the necessary stability in the blowing sub-process. Finally, the appropriate thermal profile in the blowing sub-process was performed with a heating rate of 4 ° C / s and a cooling rate of 9.5 ° C / s. Achieving the technology of making this hemispherical glass shell in sub-millimeter dimensions, which plays the role of the resonator in an HRG, due to the superior features of this gyroscope such as low noise, good performance, and long lifetime, and its application in strategic industries, like navigation and smart weapons, it is of particular importance.

## Author Contributions

All the authors participated in the conceptualization, implementation, and writing.

## Funding

The authors received no special funding for this effort.

## Acknowledgment

This work is completely self-supporting, thereby no any financial agency's role is available.

## Conflict of Interest

The authors declare no potential conflict of interest regarding the publication of this work. In addition, the ethical issues including plagiarism, informed consent, misconduct, data fabrication and, or falsification, double publication and, or submission, and redundancy have been completely witnessed by the authors.

## Abbreviations

HRG	Hemispherical Resonator Gyroscope
HSR	Hemispherical Shell Resonator

## References

- [1] A.M. Shkel, "Type I and type II micromachined vibratory gyroscopes," in Proc. IEEE/ION PLANS 2006: 586–593, 2006.
- [2] R. Sedaghati, M. Mahmoudian, "Hemispherical vibratory gyroscope performance evaluation and sensitivity analysis with capacitive excitation," J. Electr. Comput. Eng. Innovations, 7(1): 45–56, 2019.
- [3] L. Yun, L. Bing, W. Xu, W. Wenqi, "Quadrature control of hemispherical resonator gyro based on FPGA," in Proc. IEEE 2011 10th International Conference on Electronic Measurement & Instruments, 3: 369–372, 2011.
- [4] D.M. Rozelle, "The hemispherical resonator gyro: From wineglass to the planets," in Proc. 19th AAS/AIAA Space Flight Mechanics Meeting, 134: 1157–1178, 2009.
- [5] D. Senkal, A.M. Shkel, Whole-Angle MEMS Gyroscopes: Challenges and Opportunities. John Wiley & Sons, 2020.
- [6] E.C. Litty, L.L. Gresham, P.A. Toole, D.A. Beisecker, "Hemispherical resonator gyro: an IRU for Cassini," in Proc. Cassini/Huygens: A Mission to the Saturnian Systems, 2803: 299–310, 1996.
- [7] D. Meyer, D. Rozelle, "Milli-HRG inertial navigation system," Gyroscopy Navig., 3(4): 227–234, 2012.
- [8] D. Senkal, M. J. Ahamed, A. A. Trusov, A.M. Shkel, "Achieving sub-Hz frequency symmetry in micro-glassblown wineglass resonators," J. Microelectromechanical Syst., 23(1): 30–38, 2013.
- [9] L. Zeng et al., "A 5.86 million quality factor cylindrical resonator with improved structural design based on thermoelastic dissipation analysis," Sensors, 20(21): 6003, 2020.
- [10] G.H. Bryan et al., "On the beats in the vibrations of a revolving cylinder or bell," in Proc. the Cambridge Philosophical Society, 7(24): 101–111, 1890.
- [11] Y. Huo, S. Ren, Z. Wei, G. Yi, "Standing wave binding of hemispherical resonator containing first–third harmonics of mass imperfection under linear vibration excitation," Sensors, 20(19): 5454, 2020.
- [12] A.V. Vafanejad, "Wineglass mode resonators, their applications and study of their quality factor," University of Southern California, 2015.

- [13] A. Darvishian, B. Shiari, J.Y. Cho, T. Nagourney, K. Najafi, "Anchor loss in hemispherical shell resonators," *J. Microelectromechanical Syst.*, 26(1): 51–66, 2017.
- [14] E.J. Eklund, A.M. Shkel, "Glass blowing on a wafer level," *J. Microelectromechanical Syst.*, 16(2): 232–239, 2007.
- [15] R. Lutwak, "Micro-technology for positioning, navigation, and timing towards PNT everywhere and always," in Proc. 2014 International Symposium on Inertial Sensors and Systems (SISS): 1–4, 2014.
- [16] M.H. Asadian, Y. Wang, S. Askari, A. Shkel, "Controlled capacitive gaps for electrostatic actuation and tuning of 3D fused quartz micro wineglass resonator gyroscope," in Proc. 2017 IEEE International Symposium on Inertial Sensors and Systems (INERTIAL): 1–4, 2017.
- [17] J.Y. Cho, S. Singh, J.-K. Woo, G. He, K. Najafi, "0.00016 deg/v hr Angle Random Walk (ARW) and 0.0014 deg/hr Bias Instability (BI) from a 5.2 MQ and 1-cm Precision Shell Integrating (PSI) Gyroscope," in Proc. 2020 IEEE International Symposium on Inertial Sensors and Systems (INERTIAL): 1–4, 2020.
- [18] D. Senkal, M.J. Ahamed, A.A. Trusov, A.M. Shkel, "High temperature micro-glassblowing process demonstrated on fused quartz and ULE TSG," *Sensors Actuators A Phys.*, 201: 525–531, 2013.
- [19] D. Senkal, C. R. Raum, A.A. Trusov, A.M. Shkel, "Titania silicate/fused quartz glassblowing for 3-D fabrication of low internal loss wineglass micro-structures," in Proc. Solid-State Sensors, Actuators, and Microsystems Workshop 2012: 267–270, 2012.
- [20] J. Cho, J. Yan, J.A. Gregory, H. Eberhart, R.L. Peterson, K. Najafi, "High-Q fused silica birdbath and hemispherical 3-D resonators made by blow torch molding," in Proc. 2013 IEEE 26th International Conference on Micro Electro Mechanical Systems (MEMS): 177–180, 2013.
- [21] B. Li, X. Xi, K. Lu, Y. Shi, D. Xiao, X. Wu, "Frequency split suppression of fused silica micro shell resonator based on rotating forming process," *Microsyst. Technol.*: 1–11, 2020.
- [22] A. Darvishian, T. Nagourney, J.Y. Cho, B. Shiari, K. Najafi, "Thermoelastic dissipation in micromachined birdbath shell resonators," *J. Microelectromechanical Syst.*, 26(4): 758–772, 2017.
- [23] A. Heidari et al., "Micromachined polycrystalline diamond hemispherical shell resonators," in Proc. 2013 Transducers & Eurosensors XXVII: The 17th International Conference on Solid-State Sensors, Actuators and Microsystems (TRANSDUCERS & EUROSENSORS XXVII): 2415–2418, 2013.
- [24] D. Senkal, M.J. Ahamed, A.M. Shkel, "Design and modeling of micro-glassblown inverted-wineglass structures," in Proc. 2014 International Symposium on Inertial Sensors and Systems (SISS): 1–4, 2014.
- [25] J.Y. Cho, K. Najafi, "A high-q all-fused silica solid-stem wineglass hemispherical resonator formed using micro blow torching and welding," in Proc. 2015 28th IEEE International Conference on Micro Electro Mechanical Systems (MEMS): 821–824, 2015.
- [26] J.Y. Cho, J. Yan, J.A. Gregory, H.W. Eberhart, R.L. Peterson, K. Najafi, "3-dimensional blow torch-molding of fused silica microstructures," *J. Microelectromechanical Syst.*, 22(6): 1276–1284, 2013.
- [27] L. Sorenson, F. Ayazi, "Effect of structural anisotropy on anchor loss mismatch and predicted case drift in future micro-hemispherical resonator gyros," in Proc. IEEE/ION PLANS 2014: 493–498, 2014.
- [28] A. Vafanejad, E.S. Kim, "Sub-degree angle detection using dome-shaped diaphragm resonator with wine-glass mode vibration," in Proc. Hilton Head: 391–394, 2014.
- [29] B. Luo, J. Shang, Z. Su, J. Zhang, C.-P. Wong, "Height adjustment of 3-D axisymmetric microcumbrella shells for tailoring wineglass frequency," *IEEE Trans. Components, Packag. Manuf. Technol.*, 9(3): 567–574, 2018.
- [30] A. Matthews, "An operation and mechanization of the hemispherical resonator gyroscope," in Proc. 2018 IEEE/ION Position, Location and Navigation Symposium (PLANS): 7–14, 2018.
- [31] D. Senkal, "Micro-glassblowing Paradigm for Realization of Rate Integrating Gyroscopes," UC Irvine, 2015.
- [32] B. Luo, J. Shang, Y. Zhang, "Hemispherical glass shell resonators fabricated using Chemical Foaming Process," in Proc. 2015 IEEE 65th Electronic Components and Technology Conference (ECTC): 2217–2221, 2015.
- [33] R. Wang et al., "Design and fabrication of micro hemispheric shell resonator with annular electrodes," *Sensors*, 16(12): 1991, 2016.
- [34] J. Giner, A.M. Shkel, "The concept of "collapsed electrodes" for glassblown spherical resonators demonstrating 200: 1 aspect ratio gap definition," in Proc. 2015 IEEE International Symposium on Inertial Sensors and Systems (SISS): 1–4, 2015.
- [35] D. Senkal, M.J. Ahamed, S. Askari, A. M. Shkel, "1 million Q-factor demonstrated on micro-glassblown fused silica wineglass resonators with out-of-plane electrostatic transduction," in Proc. Hilton Head Workshop: 68–71, 2014.
- [36] M. Kanik et al., "Metallic glass hemispherical shell resonators," *J. Microelectromechanical Syst.*, 24(1): 19–28, 2014.
- [37] Z. Su, J. Shang, B. Luo, C.-P. Wong, "Study on an Improved Wafer Level Fabrication Process to Achieve Size Uniformity for Micro Glass Shell Resonators," in Proc. 2018 IEEE 68th Electronic Components and Technology Conference (ECTC): 962–966, 2018.
- [38] W. Li et al., "Application of micro-blowtorching process with whirling platform for enhancing frequency symmetry of microshell structure," *J. Micromechanics Microengineering*, 28(11): 115004, 2018.
- [39] Y. Shi et al., "Wafer-level fabrication process for micro hemispherical resonators," in Proc. 2019 20th International Conference on Solid-State Sensors, Actuators and Microsystems & Eurosensors XXXIII (TRANSDUCERS & EUROSENSORS XXXIII): 1670–1673, 2019.
- [40] P. Pai, F.K. Chowdhury, C.H. Mastrangelo, M. Tabib-Azar, "MEMS-based hemispherical resonator gyroscopes," in Proc. SENSORS IEEE, 2012: 1–4, 2012.
- [41] P. Taheri-Tehrani et al., "Micro-scale diamond hemispherical resonator gyroscope," in Proc. Hilton Head Workshop: 289–292, 2014.
- [42] J.J. Bernstein et al., "High Q diamond hemispherical resonators: fabrication and energy loss mechanisms," *J. Micromech. Microeng.*, 25(8): 85006, 2015.
- [43] L.D. Sorenson, X. Gao, F. Ayazi, "3-D micromachined hemispherical shell resonators with integrated capacitive transducers," in Proc. 2012 IEEE 25th International Conference on Micro Electro Mechanical Systems (MEMS): 168–171, 2012.

## Biographies



**Aylar Khooshehmehri** received the B.Sc. degree in Electrical Engineering from K. N. Toosi University of Technology, Tehran, Iran, in 2007. Also, she received the M.Sc. and Ph.D. degree in Electrical Engineering from Malek-Ashtar University of Technology in 2011 and 2018, respectively. Her research interests include superconducting amplifying and detector devices, MEMS, and semiconductor field effect devices.



**Abdollah Eslami Majd** was born in Hamadan, Iran, on March 23, 1976. He received the B.E. degree in applied physics from bu-ali Sina University, Hamadan, Iran in 1998. He received M.E. degree in atomic and molecular physics from Amir kabir University of Technology Tehran Polytechnic, Tehran, Iran in 2001. He received the Ph.D. Degree in photonics from laser and plasma Institute of Shahid Beheshti University, Tehran, Iran in 2011. Since joining electrical engineering and electronic department of Malek Ashtar University of

Technology in 2012, he has engaged in research and development of stary light in the satellite camera, laser induced breakdown spectroscopy (LIBS) and hemispherical resonator gyroscope (HRG). He is co-author of more than 30 publications. Dr. Eslami is a member of Optics and Photonics Society of Iran and Physics Society of Iran.

**Seyede Atieh Hosseini** is a graduate of Malek-Ashtar University of Technology in the field of electrical engineering majoring in electronics at the master's level.

#### Copyrights

©2022 The author(s). This is an open access article distributed under the terms of the Creative Commons Attribution (CC BY 4.0), which permits unrestricted use, distribution, and reproduction in any medium, as long as the original authors and source are cited. No permission is required from the authors or the publishers.



#### How to cite this paper:

A. Khooshehmehri, A. Eslami Majd, S.A. Hosseini, "Design and fabrication of hemispherical shell resonator by glass blowing method," J. Electr. Comput. Eng. Innovations, 10(1): 37-46, 2022.

**DOI:** [10.22061/JECEI.2021.7759.429](https://doi.org/10.22061/JECEI.2021.7759.429)

**URL:** [https://jecei.sru.ac.ir/article\\_1555.html](https://jecei.sru.ac.ir/article_1555.html)

